

Heat Transport in a Two-Dimensional Complex (Dusty) Plasma at Melting Conditions

V. Nosenko, S. Zhdanov, A. V. Ivlev, and G. Morfill

Max-Planck-Institut für extraterrestrische Physik, D-85741 Garching, Germany

J. Goree

Department of Physics and Astronomy, The University of Iowa, Iowa City, Iowa 52242, USA

A. Piel

Institut für Experimentelle und Angewandte Physik, Christian-Albrechts Universität, Kiel, Germany

(Received 22 June 2007; published 17 January 2008)

The heat transport in a two-dimensional complex (dusty) plasma undergoing a phase transition was studied experimentally. A single layer of highly charged polymer microspheres was suspended in a plasma sheath. A part of this lattice was heated by two counterpropagating focused laser beams that moved rapidly around in the lattice and provided short intense random kicks to the particles. Above a threshold, the lattice locally melted. The spatial profiles of the particle kinetic temperature were analyzed to find a thermal conductivity, which did not depend on temperature.

DOI: [10.1103/PhysRevLett.100.025003](https://doi.org/10.1103/PhysRevLett.100.025003)

PACS numbers: 52.27.Lw, 52.27.Gr

Thermal conductivity is an important property of matter. It is essential in many engineering applications. On the other hand, the behavior of thermal conductivity in various situations can give an insight into fundamental processes that occur at the atomistic (kinetic) level. The thermal conductivity of a solid or a liquid can (in principle) be measured experimentally. These experiments, however, can only be performed at a macroscopic scale and cannot resolve the details of the heat transfer processes at an atomistic level. The obvious reason for this is the lack of experimental techniques to study the motion of individual atoms or molecules in regular matter at relevant space and time scales. Therefore, an experimental model system where the motion of individual “atoms” can be observed in real time is highly desirable.

A suitable model system to experimentally study heat transport at an atomistic level is a complex (dusty) plasma [1]. A complex plasma is an ionized gas that has small particles of solid matter in it. Micron-size particles carry a large negative charge because they absorb more electrons than ions from plasma. Because of a balance of several forces (including electric, ion drag, gravity, neutral-gas drag, and thermophoretic forces) particles can be confined in a plasma region. Then the mutual interaction of the particles causes them to self-organize in a structure, termed a “plasma crystal,” that can have a crystalline or liquid order. In this plasma crystal, the interparticle distance is of the order of 0.1–1 mm and characteristic frequencies are of the order of 1–100 Hz, making it possible to observe the motion of individual atoms in real time.

Two-dimensional (2D) complex plasmas that can form in the presence of gravity are an especially attractive model system to study various phenomena at an atomistic level. In a 2D complex plasma, a fully resolved dynamics of particles can be observed, providing a complete kinetic de-

scription of experimental system. Complex plasmas were successfully used to study wave propagation [2,3], phase transitions [4], and transport phenomena [5] in 2D geometry.

To our knowledge, so far the heat transport in 2D systems was mostly studied in crystalline lattices, not liquids. For liquids, published work includes a simulation of frictionless hard disks [6] where the thermal conductivity slowly diverged in the thermodynamic limit, and theoretical study [7] where a lack of a valid thermal conductivity was conjectured. Systems undergoing a phase transition were not studied, to our knowledge.

In the present Letter, we experimentally study the heat transport in a 2D complex plasma that is undergoing a phase transition and therefore constitutes a mixture of crystalline and liquid phases. Heat transport at melting conditions is essential in material processing, crystal growth [8], and pattern formation [9]. In regular matter, the thermal conductivity (unlike self-diffusion and viscosity) does not exhibit any major discontinuity at the liquid-solid phase boundary [10]; using complex plasmas, this prediction can be verified at kinetic level. Note that published experiments on the heat transport in 2D complex plasmas are limited to crystalline phase [11]; no data are available for a liquid or melting 2D complex plasma. The heat transport in a liquid complex plasma was studied only in 3D geometry [12] that cannot be directly compared to our 2D system.

Our experimental setup was as in Ref. [13], using similar experimental parameters. Argon plasma was produced using a capacitively-coupled rf discharge. We used 31 W of rf power at 13.56 MHz, with an amplitude of 144 V peak to peak. The self-bias voltage was -88 V. To reduce the gas friction, Ar was used at a relatively low pressure of 5 mTorr. The neutral-gas damping rate is then accurately

modeled [14] by the Epstein expression $\nu = \delta N_g m_g \bar{v}_g (\rho_p r_p)^{-1}$, where N_g , m_g , and \bar{v}_g are the number density, mass, and mean thermal speed of gas atoms and ρ_p , r_p are the mass density and radius of the particles, respectively. With leading coefficient $\delta = 1.26$ [14], this gave $\nu = 0.87 \text{ s}^{-1}$, so that particle motion on the time scales studied here was not overdamped.

A single layer of microspheres was suspended in the plasma. The particles were highly charged and levitated against gravity in the sheath above the lower rf electrode. The particles had a diameter of $8.09 \pm 0.18 \text{ }\mu\text{m}$ [14] and a mass $m = 4.2 \times 10^{-13} \text{ kg}$. The suspension with a diameter D of 50–60 mm included ≈ 5000 particles and rotated slowly in the horizontal plane. The interparticle spacing measured from the pair correlation function $g(r)$ varied from 0.69 mm in the suspension center to 0.76 mm in its periphery.

The particles were imaged through the top window by a video camera. We digitized movies of 2048 frames at 29.97 frames per second. The $22.7 \times 17.0 \text{ mm}^2$ field of view included ≈ 900 particles. The particle coordinates x , y and velocities v_x , v_y were then calculated with subpixel resolution [15] for each particle in each frame.

At our experimental conditions, the particle suspension self-organized in a highly ordered triangular lattice. The interparticle potential for this lattice is well approximated [16] by the Yukawa potential: $U(r) = Q(4\pi\epsilon_0 r)^{-1} \times \exp(-r/\lambda)$, where Q is the particle charge and λ is the screening length. We used the pulse technique of Ref. [17], making use of a theoretical wave dispersion relation [18], to measure $Q = (-12200 \pm 1100)e$ and $\lambda = 0.82 \pm 0.12 \text{ mm}$. The compressional and shear waves had the sound speeds $C_L = 28.7 \pm 2 \text{ mm/s}$ and $C_T = 5.4 \pm 0.5 \text{ mm/s}$, respectively.

We used the laser-heating method of Ref. [13] to melt the lattice locally and to control the temperature of the resulting liquid complex plasma. Two laser beams with a wavelength of 532 nm were pointed toward the suspension from opposite sides at a grazing angle. Particles were pushed by the radiation pressure force. The laser beams were moved about using scanning mirrors, so that the beam footprints drew Lissajous figures on the suspension with the frequencies of $f_x = 9 \text{ Hz}$ and $f_y = 14.5623 \text{ Hz}$. To produce temperature gradients that are mainly one-dimensional, with temperature varying mostly in the y direction, we heated a narrow area, 12 mm width in the y direction, which extended fully across the suspension in the x direction.

The particle motion induced by the laser heating had two main components: regular motion (average flow and waves) and random motion. The average particle flow was the slowest component, with the typical velocity range of $\approx 0.1\text{--}0.3 \text{ mm/s}$ and the scale length of $\approx 5 \text{ mm}$. Compressional waves were excited in the laser-heating area and propagated across the particle suspension; these had the typical amplitude of $\approx 0.5 \text{ mm/s}$ and scale length

of $\approx 3\text{--}4 \text{ mm}$. The random particle motion had instantaneous velocities exceeding 1–2 mm/s.

Under these conditions, heat was mainly transferred by thermal conductivity in the region where the temperature gradient was high. The role of waves was to raise the background temperature level due to the viscous conversion of the wave energy into heat.

We calculated the particle kinetic temperature using the following method. Every frame was divided into 80 rectangular bins, arranged in the 5 by 16 grid in the x and y directions, respectively. The bin size was chosen so that we can calculate the mean kinetic energy after subtracting the mean velocity in each bin. In every bin, the velocity distribution of the random particle motion was close to Maxwellian, as shown in the insets of Fig. 1 (these distributions include data for all 2048 frames). Therefore, we calculated the particle temperature in every bin as $m\langle(v_{x,y} - \bar{v}_{x,y})^2\rangle/k_B$, where v_x and v_y are respective components of the particle velocity. Then we averaged these values in each bin over all frames of our data; this gave the averaged temperature $T_{x,y}$ as a function of x and y . This method significantly reduced the effect of pixel locking [13] on the calculated values of $T_{x,y}$.

The particle temperature was anisotropic, $T_x \neq T_y$ (see insets of Fig. 1). In the laser-heated area, $T_x = (1.1\text{--}1.2)T_y$, due to the laser-beam configuration [13]. Far from the heated area, $T_x = (0.5\text{--}0.6)T_y$; here, we attribute the temperature anisotropy to the viscous heating of particles by the waves propagating from the heated area mostly in the y direction. Just outside of the heated area, $T_x \approx T_y$. Below, we analyze the averaged temperature $T = (T_x + T_y)/2$.

The steady-state profile of the averaged particle temperature is shown in Fig. 1. The temperature was the highest in the laser-heating area and diminished away from it. As expected, the temperature profile was essentially one-dimensional, with no significant variation with x .

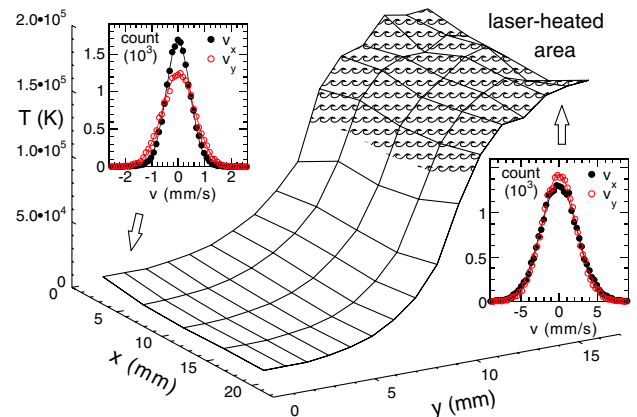


FIG. 1 (color online). Steady-state profile of the averaged particle temperature $T = (T_x + T_y)/2$ at the highest heating laser power of 16 W. Two heating laser beams were parallel to the x axis. Insets show the particle velocity distributions; solid lines indicate Maxwellian fits.

For every value of y , we averaged the particle temperature in the three x -bins that were the farthest from the crystal edge ($x > 9$ mm), to arrive at the $T(y)$ spatial profiles.

In Fig. 2(a), the particle temperature profiles $T(y)$ are shown for different values of the heating laser power. Our particle suspension melts in this temperature range, as it follows from the analysis of the pair correlation function $g(r)$. Far from the laser-heated area, $g(r)$ has the appearance characteristic of the solid phase [13], notably many peaks and the first peak amplitude of 4.8–6.5, as shown in Fig. 2(b). Inside the laser-heated area, $g(r)$ is typical for a liquid phase, including few peaks and the first peak amplitude of 1.6–2.6, as shown in Fig. 2(c). According to the Kosterlitz-Thouless-Halperin-Nelson-Young (KTHNY) theory [19], a 2D solid melts via two 2nd-order phase transitions. Estimates show that in our case these transitions occur at the temperature of $\approx 8.2 \times 10^4$ K [20] and $\approx 1.2 \times 10^5$ K [21]. (Note that the KTHNY theory does not deal with any heterogeneous structures that may exist in the melting region, e.g., domain walls.)

Outside of the laser-heated area, the temperature profiles were well approximated by exponential decay, as shown in Fig. 3. Here, we plotted the derivative dT/dy , which has the same gradient length as the temperature itself, but is not sensitive to the nearly constant background temperature T_b . The gradient length in $dT/dy \propto \exp(y/L_{\text{heat}})$ has the meaning of the heat transport length L_{heat} . From fits in Fig. 3, we derived the values of L_{heat} .

We model the steady-state temperature profiles (outside of the laser-heated area) assuming *locality* of the heat

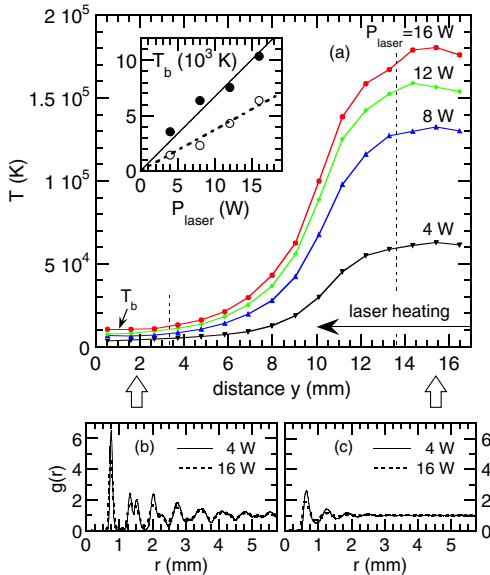


FIG. 2 (color online). (a) Particle temperature profiles as a function of the transverse coordinate y , for different values of the heating laser power P_{laser} . Inset shows background particle temperature T_b as a function of P_{laser} (solid circles) and its estimate assuming viscous heating (open circles). Pair correlation function $g(r)$ is shown (b) far from the heated stripe ($y < 3.4$ mm) and (c) inside the heated stripe ($y > 13.6$ mm).

transport and hence using the following fluid equation: $cn\mathbf{v} \cdot \nabla T k_B = \text{div}(\kappa \nabla T) - 2\gamma n(T - T_0)k_B + S_{\text{viscous}}$. Here, κ , c , n , and \mathbf{v} are, respectively, the thermal conductivity, specific heat, areal number density, and flow velocity of our particle suspension; γ is the gas friction. The temperature of our plasma crystal without laser heating is $T_0 \approx 800$ K. The term in the left-hand side of this equation describes convective heat transfer; the first and second terms in the right-hand side describe, respectively, thermal conduction and the particle kinetic energy dissipation due to the neutral-gas friction. The heat source term $S_{\text{viscous}} = (\eta/2)(\partial v_i/\partial x_k + \partial v_k/\partial x_i)^2$, where η is the shear viscosity, describes the viscous conversion of the kinetic energy of particle directed motion into heat [22].

For our experimental conditions, the heat transport equation is reduced to $\text{div}(\kappa \nabla T) = 2\gamma n(T - T_b)k_B$. Here, we omitted the convective term because it was small, contributing only less than 10% to the heat balance. The resultant action of the heat source term S_{viscous} is to raise the background temperature T_b of the particle suspension. (Estimates using the shear viscosity measured under similar conditions [5] account for $\approx 0.5T_b$; see inset of Fig. 2(a). This may mean that other heating mechanisms are at work [23].) Next, taking into account the nearly exponential spatial profiles of the particle temperature, we obtain for the thermal conductivity: $\kappa = 2\gamma n L_{\text{heat}}^2 k_B$. This formula allows us to calculate the thermal conductivity of our particle suspension from the experimentally measured heat transport length L_{heat} .

The heat transport length L_{heat} is shown in Fig. 4 as a function of the maximum temperature achieved in the laser-heated area. For comparison, we also show the phonon decay lengths due to the gas friction, for longitudinal $L_L = C_L/\gamma$ and transverse $L_T = C_T/\gamma$ phonons, as well as the average diameter of the plasma crystal D . The heat transport length turns out to be the smallest “macroscopic” scale length here: $L_{\text{heat}} < L_T < L_L$. This is a remarkable result, as it shows that the phonon scattering is not affected by the gas friction.

Our initial assumption about the locality of heat transport requires the scale characterizing inelastic phonon

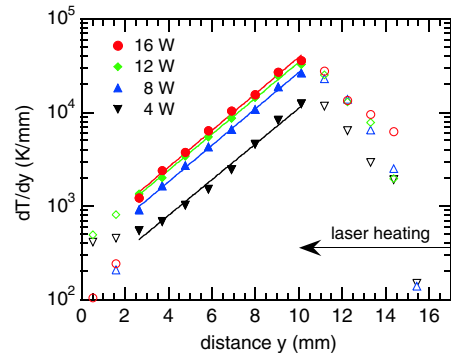


FIG. 3 (color online). Exponential fit of the temperature profiles outside of the laser-heated area. Plotted is dT/dy ; the temperature itself has the same gradient length.

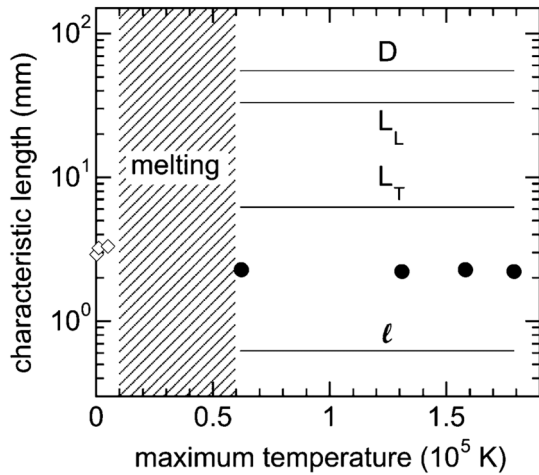


FIG. 4. Heat transport length L_{heat} as a function of the maximum temperature (solid circles—present experiment; open diamonds—Ref. [11]). The range of melting temperature is estimated based on the analysis of $g(r)$ as in Fig. 2. Various scale lengths are explained in the text.

interactions—the effective mean free path of phonons ℓ —to be smaller than any macroscopic scale of the problem. The phenomenological definition of the (2D) thermal conductivity is $\kappa \approx \frac{1}{2}cnC_{\text{eff}}\ell k_B$, where C_{eff} is the effective phonon speed. Taking into account that $C_L \gg C_T$ and assuming the equipartition of energy distribution between the two acoustic modes, we conclude that $C_{\text{eff}} \approx C_L$. This yields $\ell \approx 4L_{\text{heat}}^2/L_L \approx 0.6$ mm (Fig. 4), making our approach well justified. (We assume the regular value for the specific heat $c = 1$ [11,12].)

Thus, the heat transport in our system that undergoes a phase transition turns out to be rather simple. First, a single exponential curve fits well the spatial temperature profile in a region that comprises both liquid and solid phases (see Figs. 2 and 3). It is well known that in regular matter the thermal conductivity κ (unlike self-diffusion and viscosity) does not exhibit any major discontinuity at the liquid-solid phase boundary [10]; here, we verify this conclusion for a 2D complex plasma. Second, the values of κ calculated for different particle temperatures are almost the same. This result is not trivial, as individual phases, solid and liquid, are expected to have a temperature-dependent thermal conductivity. We speculate that the mechanism of thermal conduction in our system is phonon scattering on fluctuations that occur in the melting region (e.g., dynamical heterogeneities [24]).

Finally, we estimate the thermal diffusivity of our complex plasma near melting transition as $\chi \equiv \kappa/cn = 2\gamma L_{\text{heat}}^2 k_B/c \approx 9$ mm²/s. This result is between the values of 30 mm²/s and ≈ 1 mm²/s reported for experiments using a 2D solid [11] and a 3D liquid complex plasma [12], respectively.

To summarize, the heat transport in a 2D complex (dusty) plasma near a melting transition was studied ex-

perimentally. Unlike some simulated equilibrium systems, the particle suspension in our experiment was a damped-driven nonequilibrium system. A finite thermal conductivity was found, which did not depend on temperature. Future work may include the study of whether the thermal conductivity depends on the system size and other experimental parameters.

The work at Iowa was supported by NASA and the U.S. Department of Energy.

-
- [1] V.E. Fortov *et al.*, Phys. Rep. **421**, 1 (2005).
 - [2] S. Nunomura, S. Zhdanov, D. Samsonov, and G. Morfill, Phys. Rev. Lett. **94**, 045001 (2005).
 - [3] V. Nosenko, J. Goree, and F. Skiff, Phys. Rev. E **73**, 016401 (2006).
 - [4] C.A. Knapek *et al.*, Phys. Rev. Lett. **98**, 015004 (2007).
 - [5] V. Nosenko and J. Goree, Phys. Rev. Lett. **93**, 155004 (2004).
 - [6] T. Shimada *et al.*, J. Phys. Soc. Jpn. **69**, 3150 (2000).
 - [7] M.H. Ernst, E.H. Hauge, and J.M.J. van Leeuwen, Phys. Rev. Lett. **25**, 1254 (1970).
 - [8] C.A. Siqueira, N. Cheung, and A. Garcia, Metall. Mater. Trans. A **33**, 2107 (2002).
 - [9] H.M. van Driel and K. Dworschak, Phys. Rev. Lett. **69**, 3487 (1992).
 - [10] N.H. March and M.P. Tosi, *Introduction to Liquid State Physics* (World Scientific Publishing, Singapore, 2002).
 - [11] S. Nunomura, D. Samsonov, S. Zhdanov, and G. Morfill, Phys. Rev. Lett. **95**, 025003 (2005).
 - [12] V.E. Fortov *et al.*, Plasma Phys. Rep. **32**, 323 (2006); V.E. Fortov *et al.*, Phys. Rev. E **75**, 026403 (2007).
 - [13] V. Nosenko, J. Goree, and A. Piel, Phys. Plasmas **13**, 032106 (2006).
 - [14] B. Liu, J. Goree, and V. Nosenko, Phys. Plasmas **10**, 9 (2003).
 - [15] D. Samsonov *et al.*, Phys. Rev. Lett. **83**, 3649 (1999).
 - [16] U. Konopka, G.E. Morfill, and L. Ratke, Phys. Rev. Lett. **84**, 891 (2000).
 - [17] V. Nosenko, J. Goree, Z.W. Ma, and A. Piel, Phys. Rev. Lett. **88**, 135001 (2002).
 - [18] X. Wang, A. Bhattacharjee, and S. Hu, Phys. Rev. Lett. **86**, 2569 (2001).
 - [19] J.M. Kosterlitz and D.J. Thouless, J. Phys. C **6**, 1181 (1973); B.I. Halperin and D.R. Nelson, Phys. Rev. Lett. **41**, 121 (1978); D.R. Nelson and B.I. Halperin, Phys. Rev. B **19**, 2457 (1979); A.P. Young, Phys. Rev. B **19**, 1855 (1979).
 - [20] F.M. Peeters and X. Wu, Phys. Rev. A **35**, 3109 (1987).
 - [21] S. Nunomura, D. Samsonov, S. Zhdanov, and G. Morfill, Phys. Rev. Lett. **96**, 015003 (2006).
 - [22] L.D. Landau and E.M. Lifshitz, *Fluid Mechanics* (Butterworth-Heinemann, Boston, 1997), Vol. 6.
 - [23] T. Bjerke, Z. Li, and J. Lambros, Int. J. Plast. **18**, 549 (2002).
 - [24] C. Reichhardt and C.J.O. Reichhardt, Phys. Rev. Lett. **90**, 095504 (2003).